

UNCLASSIFIED

Defense Technical Information Center  
Compilation Part Notice

ADP012245

TITLE: Optical Characterization and Modeling of Sulfur Incorporated  
Nanocrystalline Carbon Thin Films Deposited By Hot Filament CVD

DISTRIBUTION: Approved for public release, distribution unlimited

This paper is part of the following report:

TITLE: Nanophase and Nanocomposite Materials IV held in Boston,  
Massachusetts on November 26-29, 2001

To order the complete compilation report, use: ADA401575

The component part is provided here to allow users access to individually authored sections of proceedings, annals, symposia, etc. However, the component should be considered within the context of the overall compilation report and not as a stand-alone technical report.

The following component part numbers comprise the compilation report:

ADP012174 thru ADP012259

UNCLASSIFIED

## Optical Characterization and Modeling of Sulfur Incorporated Nanocrystalline Carbon Thin Films Deposited By Hot Filament CVD

S. Gupta<sup>a</sup>, B. R. Weiner<sup>b</sup> and G. Morell<sup>c</sup>

<sup>a</sup>Department of Physics, University of Puerto Rico, San Juan, PO Box 23343, PR00931, USA

<sup>b</sup>Department of Chemistry, University of Puerto Rico, San Juan, PO Box 23346, PR00931, USA

<sup>c</sup>Dept. of Physical Science, University of Puerto Rico, San Juan, PO Box 23323, PR00931, USA

### ABSTRACT

Sulfur incorporated nanocrystalline carbon (n-C:S) thin films grown on molybdenum substrates by hot-filament chemical vapor deposition (HFCVD) using gas mixtures of methane, hydrogen and a range of hydrogen sulfide (H<sub>2</sub>S) concentrations are optically examined using Raman spectroscopy (RS) and *ex situ* spectroscopic phase modulated ellipsometry (SPME) from near IR to near UV (1.5-5.0 eV) obtaining their vibrational frequencies and pseudodielectric function, respectively. The ellipsometry data ( $\langle\epsilon_i(E)\rangle$ ,  $\langle\epsilon_t(E)\rangle$ ) were modeled using Bruggeman effective-medium theory (BEMT) and five parameters Forouhi and Bloomer (FB) dispersion Model. A simplified two-layer model consisting of a top layer comprising an aggregate mixture of sp<sup>3</sup>C+sp<sup>2</sup>C+void and a bulk layer (L<sub>2</sub>), defined as a dense amorphized FB-modeled material was found to simulate the data reasonably well. Through these simulations, it was possible to estimate the dielectric function of our n-C: S material, along with the optical bandgap (E<sub>g</sub>), film thickness (d), and roughness layer ( $\sigma$ ) as a function of [H<sub>2</sub>S]. The physical interpretation(s) of the modeling parameters obtained were discussed. The Raman and ellipsometry results indicate that the average size of nanocrystallites in the sulfur-incorporated carbon thin films becomes smaller with increasing H<sub>2</sub>S concentration, consistent with AFM measurements. The bandgap was found to decrease systematically with increasing H<sub>2</sub>S concentration, indicating the enhancement of midgap states and sp<sup>2</sup> C network, in agreement with RS results. These results are compared to those obtained for the films grown without sulfur (n-C), in order to study the influence of sulfur addition to the CVD process. This analysis led to a correlation between the film microstructure and its electronic properties.

### INTRODUCTION

A great deal of attention has been given to diamond and diamond-like carbon (DLC) thin films since their advent owing to a wide range of desired and unique mechanical, optical and electronic properties (such as: high mechanical hardness, chemical inertness, negative electron affinity, and very high electron and hole mobilities) [1,2]. This combination of superlative properties paves their way to several potential and technological applications: optical coatings, wide-band IR transmissive windows, and flat panel displays (FPDs) to name a few [3]. It is also well known that the optical and electronic properties of these carbon materials are controlled by the ratio of sp<sup>3</sup>/sp<sup>2</sup> coordinated carbon bonds [4,5]. Films having a high fraction of sp<sup>3</sup> C exhibit a higher optical band gap and hardness as compared to films rich in sp<sup>2</sup> C. A number of theoretical studies of various hypothetical phases of carbon have been carried out predicting such behavior [4,6].

The complex refractive index,  $\tilde{n} = n - ik$ , where  $n$  is the refractive index and  $k$  the extinction coefficient, provides information about the distribution of bonding configurations and is therefore an important parameter for designing the material for specific technological applications [7]. Among several state-of-the art techniques for optical characterization,

spectroscopic ellipsometry (SE) has proved to be very influential and advantageous for the last two decades in the thin film structural analysis because of its inherent advantages and sensitivity [4,8,9]. Recent pioneer reports on the addition of sulfur in diamond as a donor dopant, both experimental and theoretical [10,11,12], stirred great interest in the diamond community. In general, the n-type dopants of diamond (like N, P and now S) have the potential to enhance the field emission properties of disordered and nanocrystalline carbon films by providing electrons close to the conduction band [3,13]. Presently the incorporation of sulfur is not to make diamond semiconducting, but rather tailor the material as viable cold cathodes [3]. It has been previously shown that structural defects such as  $sp^2$  C network yield low-field emitters [3,14], in contrast to the degradation of several other physical properties.

We have measured the dielectric function and vibrational frequencies of n-C:S thin films using SE and RS techniques as a function of  $[H_2S]$  in gas phase. This paper focuses on the determination of a reliable physical model to describe the optical properties of these materials. Utilizing Forouhi and Bloomer (FB) dispersion model [15], we performed multi-layer analysis to estimate the dielectric function of these n-C:S thin films. According to this five parameter model (A, B, C,  $n(\infty)$ , and  $E_g$ ) [15], the optical absorption in the visible range is dominated by a single type of electronic transition involving states within  $\sim 5$  eV of the Fermi level and hence should involve mostly  $\pi$ - $\pi^*$  excitations. In order to investigate the optical absorption processes in the disordered carbon material in thin film form studied hereby, fits to the pseudodielectric SE data were performed using Levenberg-Marquardt [16] algorithm while varying all the parameters to fit simultaneously both n and k spectra. Based on this model and through RS, we explained the behavior of optical bandgap and the refractive index in terms of  $sp^2$  C network and the introduction of structural defect states within the bandgap (midgap states). To the best of authors' knowledge no such studies have been performed so far.

## EXPERIMENTAL PROCEDURES

The sulfur incorporated nanocrystalline carbon thin films (n-C:S) were prepared in a custom-built HFCVD reactor, described in detail elsewhere [3,17]. These thin films were prepared on Mo Substrates using a 2%CH<sub>4</sub>:H<sub>2</sub> gas mixture with a total flow of 100 sccm which was directed through a Joule heated Rhenium (Re) filament. In order to incorporate sulfur (S) in the samples, H<sub>2</sub>S:H<sub>2</sub> gas mixture was introduced in the chamber. Several sulfur concentrations were used, ranging from 100 ppm to 500 ppm, with an interval of 100 ppm at a fixed substrate temperature of 900 °C. The substrate was maintained at 900-930 °C during the growth process and the total gas pressure was kept at 20 Torr. Real-time SE was used to calibrate the true temperature of the substrate surface [18]. The incorporation of sulfur was quantified by X-ray photoelectron spectroscopy (XPS) and amounted to be around 0.5-1.0 at.%.

Film thicknesses were around 0.5-1.0  $\mu$ m, measured mechanically using Tencor surface profilometer (Alpha Step 100). The root mean square (rms) surface roughness, average grain size and typical surface topological features were evaluated using AFM (Nanoscope IIIa, Digital Instruments Inc.). The Raman spectra were recorded using a triple monochromator (ISA Jobin-Yvon Inc. Model T64000) with around 1  $cm^{-1}$  resolution employing the 514.5 nm line of Ar<sup>+</sup> laser and a probed area of about 1-2  $\mu$ m<sup>2</sup>. The *ex situ* spectroscopic ellipsometry data were measured with a Jobin-Yvon UVISSEL phase-modulated spectroscopic ellipsometer (Model DH10) from NIR (1.5 eV) to near UV (5.0 eV) with a fixed incident angle of 68.58° from the sample normal and a spot size of 3 mm. During the analysis, the bulk optical function of the

material components of the film microstructure, including diamond component ( $sp^3C$ ) and non-diamond ( $sp^2C$ ) as glassy carbon, were taken following Collins [18].

## RESULTS AND DISCUSSION

Figure 1 shows the Raman spectra for the n-C:S thin films grown by HFCVD as a function of  $[H_2S]$  in gas phase. All of the samples were grown at a fixed substrate temperature of 900 °C. The film grown with 100 ppm  $H_2S$  shows the 1332  $cm^{-1}$  peak (fingerprint of diamond). Qualitative inspection of Fig. 1 also shows that the Raman spectra are dominated by broad features at 1150, 1340 and 1580  $cm^{-1}$ , which are typical characteristic of nanocrystalline diamond (n-D) [19] and disordered carbon [20], the last two denoted by D and G band, respectively. These latter features predominate with respect to the increase in sulfur concentration. The film grown with 100 ppm is quite similar to intrinsic material (n-C) and one can note the disappearance of diamond peak for films grown with  $H_2S$  greater than 200 ppm. The relative heights of the Raman peaks (D and G bands) differ in general. The latter features predominate at higher TS while their relative heights differ, in general. The difference among the Raman spectra can be explained by the sulfur additions. Under the specific growth conditions considered in this study, sulfur tends to introduce disorder and defects considerably, similar to nitrogen incorporation, which induces graphitization of carbon films [3,6,21,22]. Notice that the  $sp^2$  bond sites begin to diffuse and condense into clusters at high temperatures. This ability of clustering of  $sp^2$  sites while keeping the  $sp^3$  fraction fixed implies or indicates that these  $sp^2$  sites act like defects in the  $sp^3$  matrix. Predicted theoretically by Robertson *et al.* [23] that the midgap states are found for  $\pi$  states on  $sp^2$  sites, they cluster according to the deposition conditions, as the  $[H_2S]$  hereby. Changes in the surface morphological features are also apparent from AFM technique. The

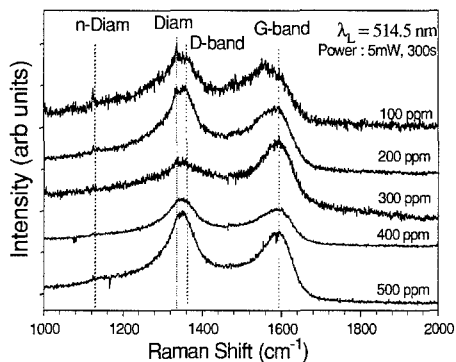


**Figure 1.** Raman spectra for S- assisted nanocrystalline carbon thin films as a function of sulfur concentration ( $[S]$ ) depicting the characteristic diamond, graphitic and disordered carbon

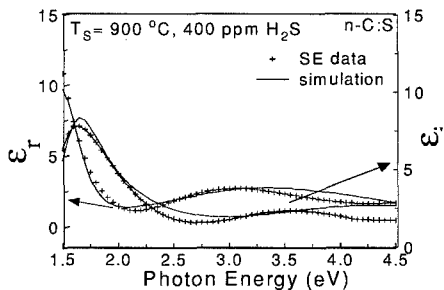


**Figure 2.** Typical *ex situ* phase modulated spectroscopic ellipsometry data for one of the sulfur-incorporated nanocrystalline carbon thin films. The crosses (+) are the raw data, while the solid line (—) is the best-fit simulation resulting from linear regression analysis (LRA) of the experimental data. The arrows indicate the two ordinates that apply to each curve.

ball-like morphology transforms to fine-grained on S-addition and the surface becomes relatively smoother ( $\sigma$ : 64 nm vs 25 nm). The average grain size estimated using AFM [3] becomes reduced from 60 to 20 nm with increasing sulfur addition. Moreover, the grain size distributions range from 20-60 nm to 100-150 nm for all of the samples. Since the Raman cross-section of graphitic carbon is around 50 times larger than that of diamond [19], there must be a substantial amount of microcrystalline diamond inclusions in the film. Besides, a substantial amount of threefold  $sp^2$  coordinated carbon ( $sp^2C$ ) is also present, indicated by the graphitic G-band at  $1580\text{ cm}^{-1}$ .

Generally speaking, the Raman band at  $1360\text{ cm}^{-1}$  has contributions from both highly defective  $sp^3$  carbon (diamond-like) and disordered  $sp^2$  carbon (graphitic D-band [20]).

The experimental *ex situ* SE data and the corresponding fits of  $\epsilon_r(E)$  and  $\epsilon_i(E)$  for one of the representative sample are shown in Fig. 2. The results were fitted employing Bruggeman Effective Medium Theory (BEMT) [24] and FB dispersion model under the assumption that the film composition is an aggregate mixture of disordered  $sp^3$  and  $sp^2$  carbon ( $sp^3C$ ,  $sp^2C$ ). For the  $sp^3$  component, the optical constants of natural type IIa diamond were adopted, while for the  $sp^2$  component the optical constants of glassy carbon were used [18]. In order to find the most appropriate one, the models having a different number of layers, different composition and two dispersion models such as Tuac-Lorenz (TL) and FB within these layers were applied to ellipsometry data. The result was that a simplified two-layer model of which the microstructural and the corresponding optical model shown in Fig. 3, was required in order to simulate the data reasonably well. This model consists of a top layer (defined as a composite layer of  $sp^3C+sp^2C+voids$ ) followed by a dense amorphized FB-modeled material layer. Last is the Mo substrate, assumed to be infinite since the light does not bounce back after passing through it. This two-layer model is in contrast to the model proposed for the material grown without sulfur (n-C), whereby the top layer consists of 50%FB+50%void [17]. The degree of agreement between the model and the ellipsometry data for n-C:S material can be evaluated from Fig. 2, where the continuous line corresponds to the simulation while the crosses correspond to the measured ellipsometry data. Both  $\epsilon_r$  and  $\epsilon_i$  were simultaneously fit using regression analysis that minimizes  $\chi^2$  [17].

Qualitatively, these are the best fits, while quantitative results are summarized in Table I. The overall thicknesses of the films derived from the SE model tally with those measured mechanically using a profilometer. The film thicknesses measured by these two techniques do agree reasonably well, thus giving another indication of the reliability of the model employed. On the other hand, the surface roughness measured by SE sometimes agrees with that estimated by AFM, but it is generally much lower. Results in terms of the bonding -antibonding state

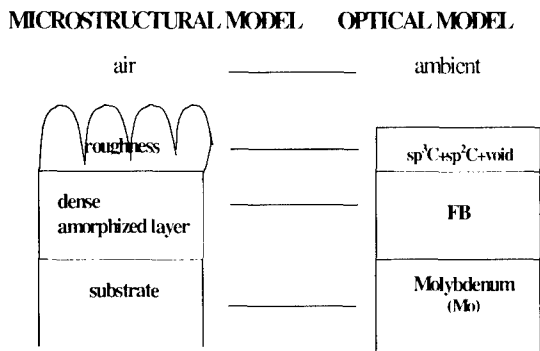


**Figure 3.** Two-layer microstructure model and the corresponding optical model to describe S-incorporated nanocrystalline carbon thin film in order to simulate the ellipsometric spectra shown in Fig. 2 for one representative sample using least-square linear regression analysis (LRA).

**Table 1.** Summary of simulation results for the sulfur-incorporated nanocrystalline carbon thin films grown by HFCVD under several hydrogen sulfide ( $\text{H}_2\text{S}$ ) concentrations in gas phase<sup>a</sup>

Sample		in gas phase						
Growth	Thickness	A	B (eV)	C (eV <sup>2</sup> )	n(∞)	E <sub>g</sub> (eV)	χ <sup>2</sup> (best-fit)	
Parameters	L <sub>2</sub> (Å)							
No sulfur	9819.3±19.7	0.190	4.108	13.916	1.714	2.701	0.16	
100 ppm	1600.1±21.5	0.27	4.586	18.73	1.52	2.18	0.29	
200 ppm	1530.4±12.4	0.25	3.921	19.30	1.91	1.15	0.89	
300 ppm	2300.2±36.9	0.60	3.510	10.71	2.20	0.92	0.18	
400 ppm	4613.7±29.5	0.94	3.506	13.36	2.97	-0.70	0.27	
500 ppm	7100.4±112.4	1.16	3.001	15.00	3.00	-1.28	1.26	

<sup>a</sup>Other deposition parameters are:  $[\text{CH}_4]=2.0\%$  in high hydrogen dilution, pressure = 20.0 Torr and number of deposition hours = 15-30 minutes for all of the samples.

$n(\infty)$  and the optical bandgap ( $E_g$ ), in agreement with the observations made for sputtered a-C and a-C:H films studied with the same model [25]. The negative values of the  $E_g$  for two of the films studied hereby seem to be unphysical but this observation is very common for these kinds of films [25] and can be overcome using modified FB model [25], which will be demonstrated in the forthcoming publication.

In the photon energy range studied hereby of 1.5-5.0 eV, the  $\pi-\pi^*$  transitions ( $\text{sp}^2$  clusters) are the predominant absorption processes involved. There are micro/nanocrystalline diamond inclusions in the film prepared with 100 ppm and, correspondingly, its bandgap is higher and the excited state lifetimes longer (smaller A) than those of the films grown with high  $\text{H}_2\text{S}$  concentration. These values then change as a result of high  $[\text{H}_2\text{S}]$ , which enhances the formation of midgap states within the band structure of the material through the formation of  $\text{sp}^2$  C bonds, resulting in lower optical bandgaps ( $E_g$ ) and shorter excited state lifetimes (larger A). These findings are in agreement with other groups concerning a-C:H deposited by PECVD with nitrogen, which leads to a strong decrease in  $E_g$ , because of the increase in aromatic regions [26]. The decrease in  $E_g$  or  $\pi-\pi^*$  transition energy confirms the nanocrystalline nature of the films, in agreement with RS. These results indicate similarities between n-C:S and n-C:N, rather than to n-C:O, and point at potential cold cathode applications of the material studied hereby.

## CONCLUSIONS

The optical properties of n-C:S thin films were investigated using RS and spectroscopic ellipsometry. A simplified two-layer structural model was found to be appropriate for simulating the ellipsometry spectra satisfactorily, obtained information about the electronic structure of these thin films. The reduction in the amount of ordered  $\text{sp}^3$  carbon was accompanied by a reduction of the effective bandgap and of the excited state lifetimes with increasing  $\text{H}_2\text{S}$  concentration in gas phase, in coordination with RS observations. Consequently, the influence of

energy difference ( $E_{\sigma\pi}-E_{\sigma\pi^*}$ ), which is a sort of average Penn gap and excited state lifetime obtained from the B and A values respectively, are listed in Table I. The findings of the optical gap  $\sim -1.28$ -2.1 eV with decreasing sulfur concentration are in agreement with the fact that the films contain a relatively high fraction of  $\text{sp}^2$  bonded carbon ( $\text{sp}^2\text{C}$ ) with increasing  $[\text{H}_2\text{S}]$ . There appears to be an inverse relation between the value of

sulfur addition to the CVD process is to increase the  $sp^2$  C content and the corresponding defect states within the bandgap. This analysis led to a correlation between the film microstructure and its electronic properties.

## ACKNOWLEDGEMENTS

One of the authors (SG) acknowledges a Graduate Research Fellowship granted by the National Science Foundation (Grant No. NSF-EPS-9874782). This research work is also supported in parts by the Department of Energy (DoE Grant No. DE-FG02-99ER45796) and NASA (Grant No. NAG5-10321). We also gratefully acknowledge the use of Micro-Raman spectroscopy facility (Dr. Ram Katiyar) in the execution of this work.

## REFERENCES

1. J. C. Angus, P. Koidl, S. Domitz, in: *Plasma Deposited Thin Films*, J. Mort, F. Jansen (Eds.), CRC Press, Boca Raton, FL, 1986, p. 89 and M. N. Yoder, in: *Synthetic Diamond: Emerging CVD Science and Technology*, K. E. Spear and J. P. Dismukes editors, (Wiley, NY, 1994), p. 4.
2. J. Robertson, *Adv. Phys.* **35**, 317 (1986).
3. S. Gupta, B. R. Weiner, B. L. Weiss and G. Morell, *Appl. Phys. Lett.* **79**, 3446 (2001) and references therein.
4. D. R. McKenzie, D. A. Muller, B. A. Paithorpe, *Phys. Rev. Lett.* **67**, 773 (1991); J. Hong, A. Goulet, and G. Turban, *Thin Solid Films* **352**, 41 (1999).
5. J. Robertson, *Philos. Mag. B* **76**, 335 (1997) and references therein.
6. D. Gruen, *Ann. Rev. Mater. Sci.* **29**, 211 (1999).
7. Z. Yin, Z. Akkerman, B. X. Yang and F. W. Smith, *Diamond & Related Mat.* **6**, 153 (1997).
8. N. Savvides, E-MRS Meeting **17**, 275 (1985); N. Savvides, *J. Appl. Phys.* **59**, 4133 (1986).
9. R. M. A. Azzam and N. M. Bashara, in *Ellipsometry and Polarized Light* (North-Holland, Amsterdam, 1977).
10. R. Kalish, A. Reznik, C. Uzan-Saguy and C. Cytermann, *Appl. Phys. Lett.* **76**, 757 (2000).
11. D. S. Dandy, *Thin Solid Films* **381**, 1 (2001).
12. M. N. Gamo, C. Xiao, Y. Zhang, E. Yasu, Y. Kikucji, I. Sakaguchi, T. Suzuki, Y. Sato and T. Ando, *Thin Solid Films* **382**, 113 (2001).
13. K. Okano, S. Koizumi, S. R. P. Silva, and G. A. J. Amartunga, *Nature*, **381**, 140 (1996).
14. J. Robertson, *Mater. Res. Soc. Symp. Proc.* **509**, 83 (1998); S. Gupta, B. L. Weiss, B. R. Weiner and G. Morell, *Mater. Res. Soc. Symp. Proc.* **638**, (2001) (in press).
15. A. R. Forouhi and I. Bloomer, *Phys. Rev. B* **34**, 7018 (1986).
16. D. W. Marquardt, *J. Soc. Indis. Appl. Math.* **11**, 431 (1963).
17. S. Gupta, B. R. Weiner and G. Morell, *Diamond and Related Materials*, **10**, 1968 (2001).
18. B. Hong, J. Lee, R. W. Collins, Y. Kuang, W. Drawl, R. Messier, T. T. Tsong and Y. F. Strausser, *Diamond and Related Materials*, **6**, 55 (1997).
19. R. J. Nemanich, J. T. Glass, G. Luckovsky and R. E. Shroder, *J. Vac. Sci. Technol. A* **6**, 1783 (1988). R. C. Hyer, M. Green, and S. C. Sharma, *Phys. Rev. B* **49**, 14573 (1994).
20. A. C. Ferrari and J. Robertson, *Phys. Rev. B* **61**, 14 095 (2000).
21. S. Bhattacharyya, K. Walzer, H. Hietschold and F. Richter, *J. Appl. Phys.* **89**, 1619 (2001).
22. R. Haubner, S. Bohr and B. Lux, *Diamond and Related Materials* **8**, 171 (2000).
23. J. Robertson and E. P. O'Reilly, *Phys. Rev. B* **35**, 2946 (1987).
24. D. A. G. Bruggeman, *Ann. Phys. Leipzig*, **24**, 636 (1935).

- 
25. W. A. McGahan and J. A. Wollam, *Mater. Res. Soc. Symp. Proc.* **349**, 453 (1994) and references therein.
  26. O. Amir, and R. Kalish, *J. Appl. Phys.* **70**, 4958 (1991).